Centrum voor Wiskunde en Informatica

REPORT*RAPPORT*

MAS

Modelling, Analysis and Simulation

Modelling, Analysis and Simulation

Population dynamics of sinking phytoplankton in stratified waters

J. Huisman, B.P. Sommeijer

REPORT MAS-R0204 FEBRUARY 28, 2002

CWI is the National Research Institute for Mathematics and Computer Science. It is sponsored by the Netherlands Organization for Scientific Research (NWO).
CWI is a founding member of ERCIM, the European Research Consortium for Informatics and Mathematics.

CWI's research has a theme-oriented structure and is grouped into four clusters. Listed below are the names of the clusters and in parentheses their acronyms.

Probability, Networks and Algorithms (PNA)

Software Engineering (SEN)

Modelling, Analysis and Simulation (MAS)

Information Systems (INS)

P.O. Box 94079, 1090 GB Amsterdam (NL)
Kruislaan 413, 1098 SJ Amsterdam (NL)
Telephone +31 20 592 9333
Telefax +31 20 592 4199

ISSN 1386-3703

Population Dynamics of Sinking Phytoplankton in Stratified Waters *

Jef Huisman †
Aquatic Microbiology, Institute for Biodiversity and Ecosystem Dynamics
University of Amsterdam
Nieuwe Achtergracht 127, 1018 WS Amsterdam, The Netherlands
jef.huisman@chem.uva.nl

Ben Sommeijer
CWI
P.O. Box 94079, 1090 GB Amsterdam, The Netherlands
bsom@cwi.nl

Abstract

We analyze the predictions of a reaction-advection-diffusion model to pinpoint the necessary conditions for bloom development of sinking phytoplankton species in stratified waters. This reveals that there are two parameter windows that can sustain sinking phytoplankton, a turbulence window and a thermocline-depth window. The two windows are delimited by four critical parameters: a minimal and maximal turbulence, and a minimal and maximal thermocline depth. Simple analytical expressions for these four critical parameters are presented, and their relation to critical parameters previously introduced by Riley, Sverdrup, and others are explained. Both parameter windows disappear if the phytoplankton sinking velocity becomes too high. This indicates the existence of a maximal phytoplankton sinking velocity that can be sustained. We derive that this maximal sinking velocity is inversely proportional to the background turbidity of the water column. In other words, clear waters can sustain species with high sinking rates, whereas turbid waters can sustain species with low sinking rates only. We demonstrate that this prediction is both qualitatively and quantitatively supported by empirical data. An intriguing implication is that export production of sinking phytoplankton can be very sensitive to the turbidity of the water column. The theory presented here offers a new framework for a better understanding of the population dynamics of sinking phytoplankton species in stratified waters.

2000 Mathematics Subject Classification: 92D25, 65M20.
1998 ACM Computing Classification System: I.6.5, J.3, G.1.7 and G.1.8.
Keywords and Phrases: Sinking Phytoplankton, Stratification, Turbidity, Export production, Numerical modelling, Integro-partial differential equation.
Note: Work carried out under subtheme MAS1.1 - Applications from the Life Sciences.

*The investigations were supported by the Earth and Life Sciences Foundation (ALW), which is subsidized by the Netherlands Organization for Scientific Research (NWO).

†Correspondence and requests for materials should be addressed to the first author.

1 Introduction

Part of the primary production in feshwater and marine ecosystems sinks to the bottom of lakes or into the deep ocean interior. Worldwide, this biological flux amounts to several gigatons of carbon per year (Falkowski et al. [18]), and acts as a major carbon sink affecting the carbon dioxide level in the atmosphere (Sundquist [57]; Sarmiento et al. [51]). A considerable fraction of the downward carbon flux consists of sinking phytoplankton species (Sancetta et al. [50]; Arrigo et al. [1]; DiTullio et al. [14]). Observational studies indicate that the abundance and distribution of sinking phytoplankton species are affected by turbulence and water column stratification (Reynolds et al. [47]; Berman and Shteinman [2]; Arrigo et al. [1]). In fact, switches in species composition from sinking phytoplankton towards neutrally buoyant or motile phytoplankton in response to changes in turbulence or stratification depth have frequently been observed (Jones and Gowen [33]; Visser et al. [61]; Sherman et al. [53]; Lauria et al. [36]; Irigoien et al. [30]). A better understanding of the population dynamics of sinking phytoplankton, in relation to turbulence and water column stratification, may therefore contribute to a better understanding of the species composition of phytoplankton communities, and of the role of sinking phytoplankton species in biogeochemical cycles.

In recent work, we derived the existence of a 'turbulence window' that enables sinking phytoplankton populations to persist (Ebert et al. [16]; Huisman et al. [25]). That is, at intermediate turbulence levels, phytoplankton populations can outgrow both mixing rates and sinking rates. As a result, the reproducing population as a whole is able to maintain a position in the euphotic zone, even if all individuals within the population have a tendency to sink. Our analysis was confined to unstratified waters, however. Although stratification of the water column is commonly regarded as a mechanism for bloom development (Sverdrup [58]; Mann and Lazier [39]), it is not clear whether stratification will keep sinking phytoplankton populations more easily within the euphotic zone. Stratification presents a barrier to turbulent motion. Thus, sinking phytoplankters may 'fall' through the pycnocline from the upper mixed layer into the deep, but the presence of a pycnocline hampers turbulent transport of sinking phytoplankton in the opposite direction (Condie [9]). One may therefore hypothesize that water column stratification restricts opportunities for blooms of sinking phytoplankton species.

Here we develop new theory to obtain a better understanding of the population dynamics of sinking phytoplankton in stratified waters. The analysis builds on previous work by, among others, Riley et al. [48], Sverdrup [58], Shigesada and Okubo [54], Smith [55], Platt et al. [43], Huisman and Weissing [29], Condie and Bormans [10], Lucas et al. [38], Huisman et al. [26, 27, 25], Diehl [12], and Ebert et al. [16]. Our approach can best be regarded as a strategic modeling approach. We are not interested in a specific ecosystem, but aim at a conceptual understanding of sinking phytoplankton in general. For this purpose, we analyze the predictions of a reaction-advection-diffusion model commonly used in aquatic ecology and oceanography (Riley et al. [48]; Koseff et al. [35]; Sharples and Tett [52]; Donaghay and Osborn [15]; Franks and Chen [19]). This model is sufficiently simple to allow mathematical tractability and general understanding, yet is sufficiently complex to incorporate the major biological-physical interactions affecting sinking phytoplankton populations.

2 The model

Model structure: We consider a vertical water column with a cross section of one unit area. The water column is stratified into two layers separated by a thermocline (Fig. 1). The depth coordinate within the water column is denoted by z, where z runs from 0 at the top to infinity at the bottom of the water column. The depth z_T indicates the position of the thermocline. We assume that the local phytoplankton dynamics are governed by growth and transport processes, where growth is determined by light availability and transport is determined by turbulence and sinking. The upper water layer is subject to turbulent mixing, whereas turbulence below the thermocline is negligibly small. Sinking phytoplankton may pass the thermocline, thereby generating export from the upper water layer into the deep waters below.

Light gradient: Let $I(z,t)$ denote the light intensity at depth z and time t, and let $\omega(z,t)$ denote the phytoplankton population density (in numbers per unit volume). According to Lambert-Beer's law, the light intensity at depth z and time t is given by (Huisman et al. [27]):

$$I(z,t) = I_{in}\, e^{-(\int_0^z k\omega(\sigma,t)d\sigma + K_{bg}z)}, \tag{1}$$

where I_{in} is the incident light intensity, k is the specific light attenuation coefficient of phytoplankton, K_{bg} summarizes the total background attenuation due to all non-phytoplankton components, and σ is an integration variable.

Population dynamics: The changes in phytoplankton population density are described by a partial differential equation (PDE):

$$\frac{\partial \omega}{\partial t} = g(I(z,t))\,\omega - v\,\frac{\partial \omega}{\partial z} + \frac{\partial}{\partial z}\left(D(z)\frac{\partial \omega}{\partial z}\right). \tag{2}$$

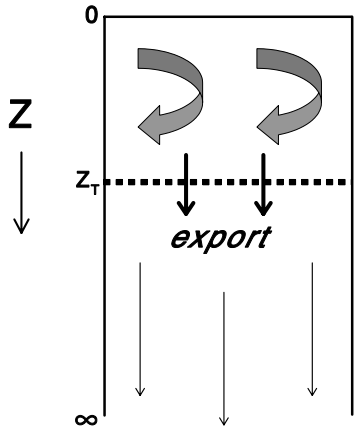

Figure 1: Model structure. The dashed line at depth z_T indicates the position of a thermocline. Above the thermocline, transport of phytoplankton is governed by turbulence and sinking. Below the thermocline, turbulence is assumed negligible, and transport of phytoplankton is governed by sinking only. The downward flux of phytoplankton over the thermocline is called export production.

Here $g(I(z,t))$ is the specific growth rate of the phytoplankton as a function of the local light intensity $I(z,t)$, v is the sinking velocity of phytoplankton, and $D(z)$ is the turbulent diffusion coefficient as a function of depth. We assume that only the upper water layer is subject to turbulent mixing, whereas turbulence is negligible in the deeper water layer. Accordingly, we set the turbulent diffusion coefficient at a uniform value $D(z) = D$ above the thermocline, and we set $D(z) = 0$ below the thermocline.

The specific growth rate in (2) depends on the balance between production and losses:

$$g(I) = p(I) - \ell, \tag{3}$$

where $p(I)$ is the specific production rate as an increasing function of light intensity, with $p(0) = 0$, and ℓ is the specific loss rate. The compensation light intensity, I_C, is defined as the light intensity at which specific production equals specific losses. That is, $g(I_C) = 0$. The corresponding point at the depth-axis is called the compensation depth.

Many alternative expressions for the $p(I)$-function are available (Jassby and Platt [31]). In all our simulations, we used Monod's [41] equation:

$$p(I) = \frac{p_{max} I}{H + I}, \tag{4}$$

where p_{max} is the maximum specific production rate and H is a half-saturation constant. We emphasize, however, that the mathematical derivations in this manuscript do not depend on the exact expression describing the $p(I)$-relationship.

Boundary conditions: Let $J(z,t)$ denote the flux of phytoplankton at depth z and time t:

$$J(z,t) = v\,\omega(z,t) - D(z)\,\frac{\partial \omega}{\partial z}(z,t). \tag{5}$$

We assume that there is no influx or efflux of phytoplankton at the water surface:

$$J(0,t) = v\,\omega(0,t) - D\,\frac{\partial \omega}{\partial z}(0,t) = 0. \tag{6}$$

Phytoplankton may sink through the thermocline, from the upper water layer into the lower water layer. Since turbulent diffusion below the thermocline is assumed negligible, the flux within the lower layer is given by the product $v\,\omega$. Hence, assuming continuity of the flux, the flux of phytoplankton at the thermocline, $J(z_T,t)$, equals:

$$J(z_T,t) = v\,\omega(z_T,t). \tag{7}$$

The flux of sinking phytoplankton at the thermocline will be called 'export production'.

We note that a boundary condition at the bottom of the (infinite) water column is not required, since the assumption that $D(z) = 0$ in the lower water layer reduces (2) to a first-order PDE with respect to z.

Table 1: Parameters used in the simulations. Phytoplankton parameters are chosen within the typical ranges measured for freshwater phytoplankton species in the culture collection of the Laboratory of Aquatic Microbiology, University of Amsterdam, The Netherlands (e.g. Visser et al. [62]; De Nobel et al. [11]; Huisman [24]; Huisman et al. [26]).

Symbol	Meaning	Value	Units
Variables			
I	light intensity		μmol photons $\cdot m^{-2} \cdot s^{-1}$
J	vertical flux of phytoplankton		cells $\cdot m^{-2} \cdot h^{-1}$
ω	population density		cells $\cdot m^{-3}$
W_T	population size per unit surface area in the upper water layer		cells $\cdot m^{-2}$
Parameters			
D	turbulent diffusion	1	$cm^2 \cdot s^{-1}$
H	half-saturation constant of light-limited growth	30	μmol photons $\cdot m^{-2} \cdot s^{-1}$
I_{in}	incident light intensity	350	μmol photons $\cdot m^{-2} \cdot s^{-1}$
K_{bg}	background turbidity	0.2	m^{-1}
k	specific light attenuation of phytoplankton	$15 \cdot 10^{-12}$	$m^2 \cdot$ cell^{-1}
ℓ	specific loss rate	0.01	h^{-1}
p_{max}	maximal specific production rate	0.04	h^{-1}
v	vertical velocity	0.04	$m \cdot h^{-1}$
z_T	thermocline depth	20	m

Population above the thermocline: It turns out useful to keep track of the total phytoplankton population within the upper water layer. According to (2) and the boundary conditions in (6) and (7), the total population within the upper water layer, $W_T(t)$, changes in time according to:

$$\frac{dW_T}{dt} = \int_0^{z_T} \frac{\partial \omega}{\partial t} dz = \int_0^{z_T} g(I(z,t))\omega(z,t)dz - v\ \omega(z_T,t). \tag{8}$$

Numerical simulations: The model predictions are analyzed using a combination of analytical and numerical techniques. The combination of (1) and (2) yields an integro-PDE, which is quite nasty to simulate numerically. Our numerical simulations are based on a finite volume method, with spatial discretization of the integro-PDE using an upwind method. The resulting stiff ODE system is integrated over time using implicit integration techniques (Brown et al. [7]). Huisman and Sommeijer [28] give a detailed account of the simulation techniques. The parameter values used in the simulations were chosen as realistic as possible. An overview of our default parameter values is given in Table 1.

3 Inert particles

Before analyzing sinking phytoplankton, we first investigate the fate of sinking inert particles. Inert particles are particles that neither grow nor decay. That is, $g(I) = 0$. Hence, from (8), a population of sinking inert particles inoculated in the upper water layer is continuously decreasing in time, since

$$\frac{dW_T}{dt} = -v\,\omega(z_T, t) \leq 0, \tag{9}$$

with equality only if $w(z_T, t) = 0$. This equation shows that, regardless of the turbulence in the upper water layer, all sinking inert particles are eventually lost from the upper water layer. If the particles in the upper water layer are uniformly mixed, so that $\omega(z_T, t) = W_T/z_T$, then (9) simplifies to

$$\frac{dW_T}{dt} = -\frac{v}{z_T}\,W_T. \tag{10}$$

This shows that, in highly turbulent upper water layers, the flux of sinking particles over the thermocline is inversely proportional to the depth of the thermocline. Thus, we obtain:

Result 1: *(i) Ultimately, all sinking inert particles are lost from the upper water layer; (ii) if the population of sinking particles within the upper water layer is uniformly mixed, then the flux of sinking particles over the thermocline is inversely proportional to thermocline depth.*

Although an inverse relation between sinking losses and thermocline depth was proposed earlier (Smith [55]; Martin and Nokes [40]; Condie [9]), our above derivation shows that this inverse relation can be deduced from simple advection-diffusion processes. The inverse relation is supported by several experimental studies. Martin and Nokes [40] added polystyrene particles to small tanks with fluids of different densities and viscosities. Reynolds et al. [44] introduced *Lycopodium* spores in experimental channels of different depths. Visser et al. [61] inoculated the fast-sinking green alga *Scenedesmus protuberans* in large indoor plankton towers with different stratification depths. Diehl et al. [13] ran field experiments in which phytoplankton communities dominated by the diatom *Cyclotella* spp. were enclosed in plastic bags mimicking various mixing depths. All these studies found an inverse relationship between sinking losses and thermocline depth. Thus, our model predictions are consistent with observed dynamics of sinking particles.

4 Phytoplankton depth profiles

A key difference between sinking inert particles and sinking phytoplankton is that the latter reproduce in the light and suffer losses in the dark. Hence, it is tempting to suggest that sinking phytoplankton might be capable to maintain a population in the upper water layer, if their growth rates in the upper water layer exceed the losses by the downward flux. To investigate this hypothesis, this section derives stationary depth profiles of sinking phytoplankton.

A trivial solution for the stationary depth profile is that there is no phytoplankton at any depth at all. More precisely, $\omega(z,t) = 0$ for all depths z and time t is, indeed, a stationary solution of (2). In the sequel, we consider the non-trivial case in which a phytoplankton population does develop. The superscript * is used to indicate the non-trivial stationary distribution.

The slope of the stationary phytoplankton depth profile in the upper water layer is obtained by solving (2) for the stationary distribution (i.e., solving for $\partial\omega/\partial t = 0$), and subsequent integration over depth. The constant of integration is determined by the boundary condition in (6). The result is:

$$\frac{d\omega^*}{dz}(z) = -\frac{1}{D}\left[\int_0^z g(I(\sigma))\omega^*(\sigma)d\sigma - v\,\omega^*(z)\right] \quad \text{for } 0 \le z < z_T. \tag{11}$$

It follows from the stationary solution of (8) and the monotonicity of the $g(I(\sigma))$-function that the integral term in (11) is positive for $0 < z < z_T$. Hence, the slope of the depth profile above the thermocline depends on the magnitudes of the two opposing terms in (11). This reveals that population density will increase with depth if the sinking flux overrides the depth-integrated growth rate. Conversely, population density will decrease with depth if the depth-integrated growth rate overrides the sinking flux. Furthermore, the population density in the upper water layer will be uniformly distributed if turbulent diffusion overrides the difference between the depth-integrated growth rate and sinking flux.

Continuity of the flux at the thermocline yields the following continuity condition:

$$\lim_{z\downarrow z_T} v\,\omega(z,t) - D\,\frac{\partial\omega}{\partial z}(z,t) = \lim_{z\uparrow z_T} v\,\omega(z,t). \tag{12}$$

Hence, the slope of the population density distribution at the thermocline, when approached from above, is given by

$$\frac{\partial\omega}{\partial z}(z,t) = 0 \quad \text{at } z = z_T. \tag{13}$$

This shows that the phytoplankton depth profile has a zero slope at the thermocline. We note that this property holds not only in the stationary situation, but for all t.

Finally, because turbulence is zero below the thermocline, according to (2) the slope of the stationary depth profile below the thermocline is given by

$$\frac{d\omega^*}{dz}(z) = \frac{1}{v}\,g(I(z))\,\omega^*(z) \quad \text{for } z_T < z < \infty. \tag{14}$$

This term is positive if $I(z) > I_C$, and negative if $I(z) < I_C$. Thus, below the thermocline, population density increases with depth for light intensities exceeding the compensation light intensity. Conversely, population density decreases with depth for light intensities that are less than the compensation light intensity. In other words:

Result 2: *A population density maximum develops below the thermocline, if the compensation depth is located below the thermocline depth.*

Figure 2 shows a variety of phytoplankton depth profiles consistent with these derivations.

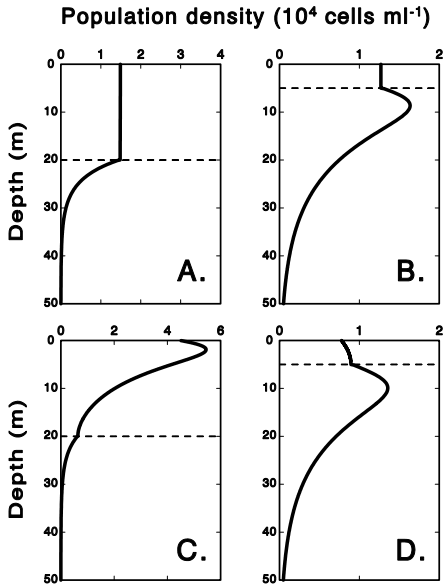

Figure 2: Stationary depth profiles of phytoplankton population density, predicted for sinking phytoplankton in (A) turbulent waters with a deep thermocline, (B) turbulent waters with a shallow thermocline, (C) quiescent waters with a deep thermocline, (D) quiescent waters with a shallow thermocline. The dashed line indicates the thermocline. Parameter values as in Table 1, except (A) $D = 1000\,cm^2 \cdot s^{-1}$, (B) $D = 1000\,cm^2 \cdot s^{-1}$, $v = 0.11\,m \cdot h^{-1}$, $z_T = 5\,m$, (C) $D = 0.5\,cm^2 \cdot s^{-1}$, (D) $D = 5\,cm^2 \cdot s^{-1}$, $v = 0.11\,m \cdot h^{-1}$, $z_T = 5\,m$.

5 Conditions for bloom development

General observations: The stationary depth profiles in Fig. 2 are all positive for at least some depth range (i.e., $W_T^* > 0$). Alternatively, the stationary population density distribution might be zero at all depths (i.e., the trivial solution $W_T^* = 0$). In the first case, we will say that there is 'bloom development', whereas in the latter case we say that there is 'no bloom'. What are the conditions favorable for bloom development of sinking phytoplankton?

In Fig. 3 we plotted the regions of bloom development and regions of no blooms for a wide range of different thermocline depths and turbulent diffusivities. This shows that sinking species neither bloom in stratified waters with a shallow thermocline (left part in Fig. 3A), nor in stratified waters with a low turbulence (lower part in Fig. 3A), nor in deeply stratified waters with a high turbulence (upper right corner in Fig. 3A). However, blooms do develop in stratified waters with an intermediate thermocline depth and/or an intermediate turbulence. The region of bloom development is bounded by nearly horizontal and vertical lines (Fig. 3A). Thus, we can recognize four critical parameters: a minimal thermocline depth, a maximal thermocline depth, a minimal turbulence, and a maximal turbulence. Below we derive analytical expressions for these four parameters.

Minimal thermocline depth: The minimal thermocline depth is hidden in the solution of the equilibrium equation $dW_T^*/dt = 0$, for a population density distribution that is

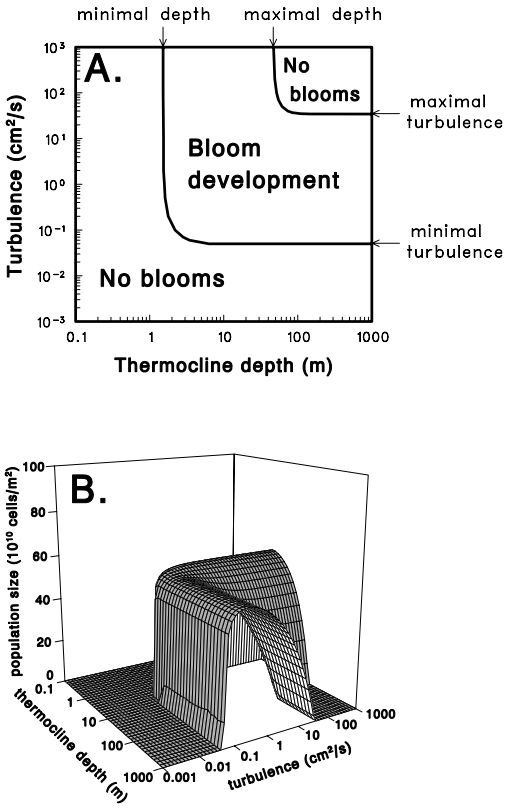

Figure 3: (A) Combinations of thermocline depth and turbulent diffusion coefficient that allow bloom development of sinking phytoplankton. (B) A three-dimensional view, in which the total population per unit surface area obtained at equilibrium is plotted as a function of thermocline depth and turbulent diffusion. The graphs are based on extensive simulations of Eqs. (1)-(8) in a grid of 41 x 61 = 2,501 simulations. Parameter values as in Table 1.

positive but negligibly small. The minimal thermocline depth occurs in turbulent waters (Fig. 3). Therefore, as a first approximation, we assume a uniform population density distribution in the upper water layer. That is, $\omega = W_T/z_T$. Hence, from (8) we obtain

$$\frac{dW_T^*}{dt} = \left[\int_0^{z_T} g(I(z))dz - v\right] \frac{W_T^*}{z_T} = 0. \tag{15}$$

The minimal thermocline depth is usually quite shallow, and phytoplankton above such a shallow thermocline will be exposed to high light intensities. Hence, especially if the specific growth rate is a saturating function of light intensity, we may use the approximation

$$\int_0^{z_{T,min}} g(I(z))dz \approx g(I_{in})\, z_{T,min}. \tag{16}$$

Substituting (16) into (15), we obtain a surprisingly simple expression for the minimal thermocline depth:

Result 3: *A necessary condition for the development of a population of sinking phytoplankton in stratified waters is that the depth of the thermocline exceeds a minimal thermocline depth. The minimal thermocline depth can be approximated as the ratio of phytoplankton sinking velocity over the specific growth rate near the surface:*

$$z_{T,min} \approx \frac{v}{g(I_{in})}. \tag{17}$$

Numerical simulations reveal that (17) provides an excellent approximation for the minimal thermocline depth in systems with low background turbidity (Fig. 4A). In systems with a high background turbidity the denominator of (17), $g(I_{in})$, overestimates the depth-averaged growth rate in the upper water layer, and as a result the minimal thermocline depth is somewhat higher than predicted by (17).

Maximal thermocline depth: To obtain an approximation for the maximal thermocline depth, the equilibrium equation (15) can be written in the following form:

$$\frac{dW_T^*}{dt} = \frac{W_T^*}{z_T} \int_0^{z_T} p(I(z))dz - \ell\, W_T^* - \frac{v}{z_T}\, W_T^* = 0. \tag{18}$$

Lambert-Beer's law, in (1), can be used to change the integral over depth in (18) into an integral over light intensity (cf. Huisman and Weissing [29]):

$$\frac{dW_T^*}{dt} = \frac{k\, W_T^*}{k\, W_T^* + K_{bg}\, z_T} \int_{I_{out,T}^*}^{I_{in}} \frac{p(I)}{kI} dI - \ell\, W_T^* - \frac{v}{z_T}\, W_T^* = 0, \tag{19a}$$

combined with

$$I_{out,T}^* = I_{in}\, e^{-(k\, W_T^* + K_{bg}\, z_T)}, \tag{19b}$$

where $I_{out,T}^*$ is the equilibrium light intensity at the thermocline.

Using a similar derivation, it can be shown that the population size per unit surface area in a well-mixed water column without stratification is hidden in the equilibrium equation (Huisman and Weissing [29]; Huisman [24]):

$$\frac{dW^*}{dt} = \frac{k\, W^*}{k\, W^* + K_{bg}\, z_m} \int_{I_{out}^*}^{I_{in}} \frac{p(I)}{kI} dI - \ell\, W^* = 0, \tag{20a}$$

combined with

$$I_{out}^* = I_{in}\, e^{-(k\, W^* + K_{bg}\, z_m)}, \tag{20b}$$

where z_m is the depth of the well-mixed water column, and I_{out}^* is known as the critical light intensity (Huisman and Weissing [29]; Huisman [24]; Huisman et al. [26]).

Let us compare the equations (19) and (20). Light intensities near the maximal thermocline depth will generally be low, and therefore the specific production rate near the thermocline will be low. Thus, it seems reasonable to assume that the total production rate integrated over the light intensities from I_{in} to $I_{out,T}^*$ in the stratified water column (19a)

is approximately equal to the total production rate integrated over the light intensities from I_{in} to I^*_{out} in the unstratified water column (20a). That is,

$$\int_{I^*_{out,T}}^{I_{in}} \frac{p(I)}{kI} dI \approx \int_{I^*_{out}}^{I_{in}} \frac{p(I)}{kI} dI. \tag{21}$$

Moreover, solving (20a) for $W^* > 0$ with the use of (20b), we obtain

$$\int_{I^*_{out}}^{I_{in}} \frac{p(I)}{kI} dI = \frac{\ell}{k} \ln\left(\frac{I_{in}}{I^*_{out}}\right). \tag{22}$$

Substituting (21) and (22) into (19a), and solving for W^*_T, yields an approximate equation for the equilibrium population size per unit surface area in a stratified water column:

$$W^*_T \approx \frac{\ln(I_{in}/I^*_{out})}{k} \frac{z_T\,\ell}{z_T\,\ell + v} - \frac{z_T}{k} K_{bg}. \tag{23}$$

Finally, setting $W^*_T = 0$ and solving for z_T yields our desired approximation for the maximal thermocline depth:

Result 4: *A necessary condition for the development of a population of sinking phytoplankton in stratified waters with a turbulent upper water layer, is that the depth of the thermocline is less than a maximal thermocline depth. The maximal thermocline depth can be approximated by the expression:*

$$z_{T,max} \approx \frac{\ln(I_{in}) - \ln(I^*_{out})}{K_{bg}} - \frac{v}{\ell}. \tag{24}$$

Simulations reveal that (24) provides an excellent approximation (Fig. 4B). Interestingly, the first term on the right-hand side of (24) is mathematically equivalent to Sverdrup's [58] critical depth (see Huisman [24]; Huisman et al. [27]). Hence, in view of the second term on the right-hand side of (24), the maximal thermocline depth for sinking phytoplankton is less deep than the critical depth predicted by Sverdrup. This discrepancy stems from losses of sinking phytoplankton over the thermocline – an aspect that was not incorporated in Sverdrup's theory. More precisely, (24) states that these sinking losses reduce the maximal thermocline depth by the ratio of sinking velocity over specific loss rate.

Minimal turbulence: Riley et al. [48, pp. 85-90] and Shigesada and Okubo [54, pp. 316-319] derived a surprisingly simple equation for the minimal turbulence, under the assumption that the vertical light gradient generated by background turbidity is negligible:

Result 5: *A necessary condition for the development of a population of sinking phytoplankton in stratified waters is that the turbulence in the upper water layer exceeds a minimal turbulence. The minimal turbulence can be approximated as the ratio of the square of sinking velocity over four times the specific growth rate near the water surface:*

$$D_{min} \approx \frac{v^2}{4\,g(I_{in})}. \tag{25}$$

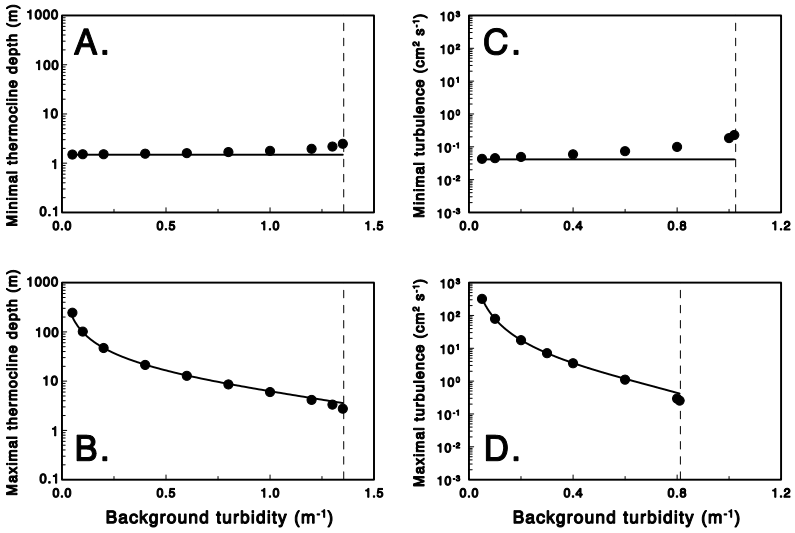

Figure 4: Suitability of analytical approximations. (A) Minimal thermocline depth predicted by the full model (dots) and by (17) (solid line). (B) Maximal thermocline depth predicted by the full model (dots) and by (24) (solid line). (C) Minimal turbulence predicted the full model (dots) and by (25) (solid line). (D) Maximal turbulence predicted by the full model (dots) and by (26) (solid line). The critical parameters vanish when background turbidity exceeds the dashed line. Parameter values as in Table 1. Using these parameter values, $I^*_{out} = 0.0124\,\mu\text{mol}\cdot m^{-2}\cdot s^{-1}$. (C) is based on the linear equation $p(I) = 0.0002\cdot I\,h^{-1}$.

Numerical simulations indicate that (25) is an accurate approximation of the minimal turbulence in systems with low background turbidity (Fig. 4C). The minimal turbulence is somewhat higher than predicted by (25) in systems with a high background turbidity.

Maximal turbulence: The maximal turbulence is equivalent to the critical turbulence discovered by Huisman et al. [27]. We have not been able to derive a simple approximation for the maximal turbulence. However, in the special case that the specific production rate is a linear function of light intensity, we were able to derive an equation for the maximal turbulence based on Bessel functions approximated by asymptotic expansion techniques. The derivation is involved, and given elsewhere (Ebert et al. [16, Eq. (94)]). Here we only state the result:

Result 6: *A necessary condition for the development of a population of sinking phytoplankton in stratified waters, with a deep thermocline, is that turbulence in the upper water layer is less than a maximal turbulence. In the special case that the specific production rate is a linear function of light intensity, $p(I) = aI$, the maximal turbulence can be approximated as:*

$$D_{max} \approx \frac{aI_{in}}{K_{bg}^2}\left(\frac{1-\gamma}{B} - \frac{(3-2\gamma)(2-\gamma)}{2(1-\gamma)} + B\,\frac{35-99\gamma+82\gamma^2-21\gamma^3}{12(1-\gamma)^3}\right), \qquad (26)$$

with dimensionless parameters $B = \ell/(aI_{in})$ and $\gamma = vK_{bg}/(aI_{in})$.

Simulations reveal that (26) is an excellent approximation for linear $p(I)$-functions (Fig. 4D). For nonlinear $p(I)$-functions, we recommend calculating the maximal turbulence by the fast algorithm outlined by Huisman et al. [25].

6 Maximal sinking velocity

General observations: Figure 5 illustrates how the critical parameters for bloom development just identified vary with the sinking velocity of phytoplankton. For neutrally

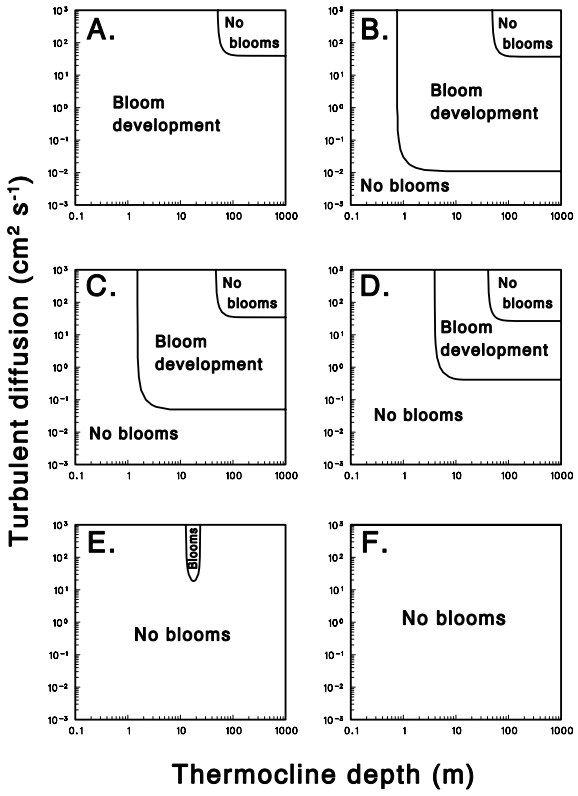

Figure 5: Bloom conditions, summarized for (A) neutrally buoyant phytoplankton, and (B-F) phytoplankton with five different sinking velocities. Each panel is based on a grid of 41 x 61 = 2,501 simulations. Parameter values as in Table 1, except (A) $v = 0\, m \cdot h^{-1}$, (B) $v = 0.02\, m \cdot h^{-1}$, (C) $v = 0.04\, m \cdot h^{-1}$, (D) $v = 0.10\, m \cdot h^{-1}$, (E) $v = 0.25\, m \cdot h^{-1}$, (F) $v = 0.40\, m \cdot h^{-1}$.

buoyant and positively buoyant species, which do not suffer from sinking losses over the thermocline, a minimal thermocline depth and minimal turbulence do not exist. Their bloom conditions are delimited by a maximal thermocline depth and maximal turbulence only (Fig. 5A). Slowly sinking species have a shallow minimal thermocline depth and low minimal turbulence (Fig. 5B). Hence, for slowly sinking species, there is still a considerable region in parameter space that allows bloom development. However, the minimal

thermocline depth and minimal turbulence both increase with increasing sinking velocity (Fig. 5C, D). At a certain sinking velocity, the minimal turbulence and maximal turbulence merge and disappear. As a consequence, species with a high sinking velocity can bloom only in turbulent environments over a narrow range of thermocline depths (Fig. 5E). If sinking velocity is increased further, the minimal and maximal thermocline depth merge as well. Hence, species with a very high sinking velocity cannot persist (Fig. 5F).

The sinking velocity at which bloom development becomes impossible throughout the D-z_T plane (i.e., the transition from Fig. 5E to Fig. 5F) will be called the 'maximal sinking velocity'.

Analytical derivations: To derive an analytical expression for the maximal sinking velocity, we introduce the growth function $G(z_T)$:

$$G(z_T) = \int_0^{z_T} g(I(z))dz. \tag{27}$$

This growth function can be substituted into the equilibrium equation (15), which then reads:

$$\frac{dW_T^*}{dt} = [G(z_T) - v]\,\frac{W_T^*}{z_T} = 0. \tag{28}$$

Accordingly, equilibrium solutions are given by the intersection points of the function $G(z_T)$ with the sinking velocity v.

Let us consider the qualitative shape of the function $G(z_T)$. It is obvious that $G(0) = 0$. Furthermore, using the Fundamental Theorem of Calculus, (27) reveals that $dG/dz_T = g(I(z_T))$. It follows from the definition of the compensation depth (underneath Eq. (3)), that G has a positive slope if the thermocline depth is less than the compensation depth, whereas G has a negative slope if the thermocline depth exceeds the compensation depth. The function G has a maximum at $G(z_C)$, i.e. at the point where the thermocline depth

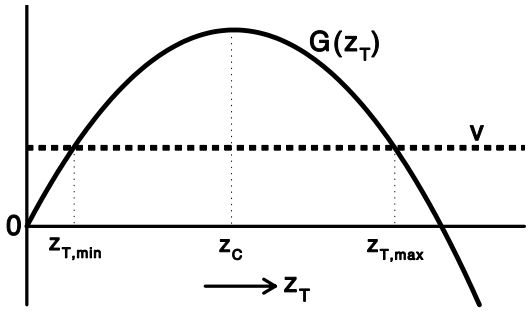

Figure 6: The growth function $G(z_T)$ and the sinking velocity v, plotted as a function of thermocline depth. Note that $G(z_T)$ and v intersect twice. The first intersection point indicates the minimal thermocline depth ($z_{T,min}$); the second intersection point indicates the maximal thermocline depth ($z_{T,max}$). The growth function $G(z_T)$ reaches a maximum at the point where the thermocline depth equals the compensation depth ($z_T = z_C$).

equals the compensation depth. Furthermore, the function G is strictly concave downward, since $d^2G/d(z_T)^2 = (dg/dI)(dI/dz_T) < 0$. This implies that G becomes negative if z_T becomes large.

The function $G(z_T)$ thus obtained is sketched in Fig. 6. The sketch shows that $G(z_T)$ and v do not intersect if $v > G(z_C)$. In this case, there is no equilibrium solution; the sinking velocity of phytoplankton is too high to sustain a population in the upper water layer. Conversely, if $0 < v < G(z_C)$, there are always two solutions of (28), at the points $z_T = z_{T,min}$ and $z_T = z_{T,max}$. These two solutions correspond to the minimal and maximal thermocline depth, respectively (Fig. 6).

The maximal sinking velocity is the sinking velocity at which the minimal and maximal thermocline depth merge. This corresponds to the point at which v equals the maximum of the growth function $G(z_T)$ (Fig. 6). Thus, the maximal sinking velocity is obtained by solving $v = G(z_T)$ at the point $z_T = z_C$. This gives:

$$v_{max} = \int_0^{z_C} g(I(z))dz. \tag{29}$$

Lambert-Beer's law, in (1), can be used to change the integration variable in (29) from an integral over depth into an integral over light intensity. We note that the population density at this bifurcation point is negligibly small (i.e., $k\,\omega^* \ll K_{bg}$). Hence, we obtain:

Result 7: *The maximal sinking velocity that can be sustained is inversely proportional to the background turbidity of the water column:*

$$v_{max} = \frac{1}{K_{bg}} \int_{I_C}^{I_{in}} \frac{g(I)}{I} dI. \tag{30}$$

More specifically, in case of the Monod equation (4), the integral in (30) can be solved and the maximal sinking velocity is given by:

$$v_{max} = \frac{1}{K_{bg}} \left(p_{max} \ln \left(\frac{H + I_{in}}{H + I_C} \right) - \ell \ln \left(\frac{I_{in}}{I_C} \right) \right). \tag{31}$$

Thus, theory predicts that clear waters can sustain phytoplankton species with a high sinking velocity. In turbid waters, only species with a low sinking velocity can persist.

Comparison with sinking-velocity data: Is the theory consistent with data? Is the maximal sinking velocity of phytoplankton inversely proportional to the background turbidity of the water column? There are a number of caveats that must be circumvented in order to evaluate this hypothesis against empirical data. First, the theory is concerned with the maximal sinking velocity. Sinking velocities of phytoplankton species can be lower than the predicted maximal velocity, but should not exceed this maximum value. Second, the theory points at the background turbidity as key parameter, not the turbidity of the water column per se. Thus, we must indeed focus on background turbidity – the turbidity generated by non-phytoplankton components. Third, the theory is concerned with sinking

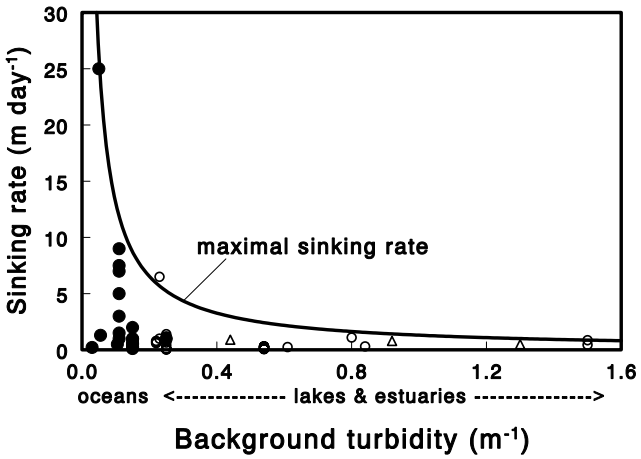

Figure 7: Sinking velocity of phytoplankton species from oceans (closed circles), estuaries and rivers (triangles), and lakes (open circles) plotted as a function of background turbidity. See Table 2 for further details of these data. The solid line is the maximal sinking velocity predicted by (31), using the parameter values of Table 1.

velocities of healthy phytoplankters under their usual growth conditions. The theory does not consider aggregates of dead phytoplankton, nor phytoplankton cells attached to fecal pellets or other sinking particles.

Though many studies report on either phytoplankton sinking velocities or background turbidities, few studies have reported on both. Table 2 shows the database that we have been able to gather so far. Despite the sparseness of the data, the data indicate clearly that the upper bound on sinking velocity decreases with increasing background turbidity. Maximal sinking velocities are typically higher in clear ocean waters than in turbid lakes and estuaries. Most strikingly, even quantitatively there is good correspondence between the sinking-velocity data (symbols in Fig. 7) and the maximal sinking velocity predicted by theory (solid line in Fig. 7). This is particularly rewarding since the model parameters (Table 1) are independent of the sinking-velocity data (Table 2). Thus, the theory appears consistent with available data.

Export production: In view of Result 7, it seems likely that the background turbidity of the water column can have quite an impact on export production. More specifically, export production is the product of population density and sinking velocity (Eq. (7)). Both the population density and the maximal sinking velocity that can be sustained vary with the background turbidity of the water column.

To explore the impact of background turbidity, Fig. 8A plots the equilibrium population size per unit surface area as a function of background turbidity and sinking velocity. The graph assumes a turbulent upper water layer and an intermediate thermocline depth. The equilibrium population size per unit surface area is a linearly decreasing function of background turbidity and a non-linearly decreasing function of sinking velocity. It turns out (not shown) that (23) provides a good approximation of the surface in Fig. 8A.

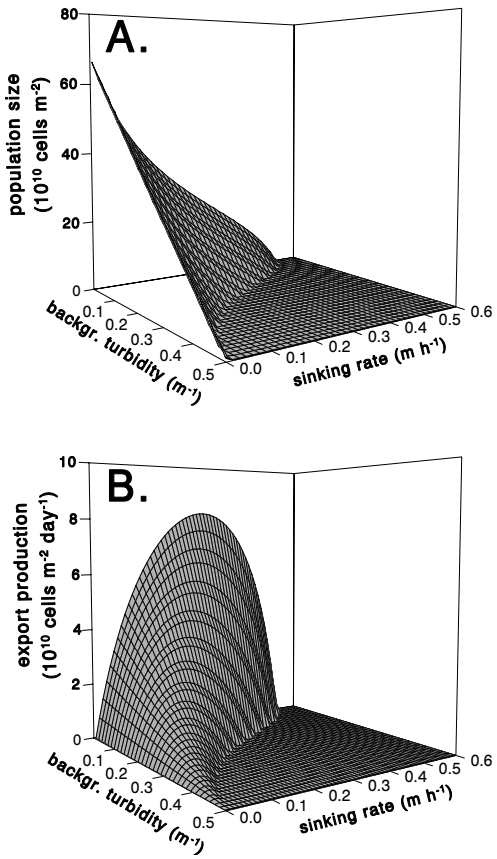

Figure 8: (A) Equilibrium population size per unit surface area in the upper water layer, and (B) equilibrium export production of sinking phytoplankton, both plotted as a function of background turbidity and sinking velocity. Graphs are based on a grid of 51 x 61 = 3,111 simulations. Parameter values as in Table 1, except $D = 200\,cm^2 \cdot s^{-1}$.

Fig. 8B shows the corresponding export production. Combining Eq. (7) and Eq. (23), for a turbulent upper water layer, the surface depicted in Fig. 8B can be approximated as

$$J^*(z_T) \approx \frac{\ln(I_{in}/I^*_{out})}{k} \, \frac{v\,\ell}{v + z_T\,\ell} - \frac{v}{k}\,K_{bg}. \tag{32}$$

This illustrates that equilibrium export production is a unimodal function of sinking velocity and a linearly decreasing function of background turbidity (Fig. 8B). Moreover, the second term on the right-hand side of (32) states that the slope of the relation between export production and background turbidity increases linearly with sinking velocity. In other words, the higher the phytoplankton sinking velocity, the stronger the negative effect of background turbidity on export production. This effect is clearly visible in Fig. 8B. Combining all this information, we arrive at the following implication:

Result 8: *Export production of sinking phytoplankton is highest for phytoplankton species with intermediate sinking velocities, in waters with a very low background turbidity.*

We emphasize that Result 8 considers export production by living phytoplankton cells only. It neglects carbon export by dissolved organic carbon, coagulated plankton aggregates, or fecal pellets – three other major components of the global carbon flux into the oceans.

7 Discussion

The ultimate fate of a sinking particle in a stratified water column is that it will be lost from the upper water layer. One of our key findings is that, despite this ultimate fate of each individual particle, populations of sinking phytoplankton can be sustained. They can be sustained if their net population growth in the upper water layer exceeds the population losses over the thermocline. More specifically, we derived two parameter windows that allow sinking phytoplankton to survive in stratified waters. One might call these windows the 'turbulence window' and 'thermocline window', respectively (Fig. 3).

We wish to emphasize that our analysis assumes that the specific growth rate of phytoplankton is determined by light availability. This implies that the parameter space that permits bloom development in our model analysis indicates the maximal parameter space for bloom development. In reality, conditions for bloom development will frequently be confined to a smaller subset within this parameter regime, because of nutrient limitation, virus attack, or zooplankton grazing. However, conditions for bloom development can never exceed the maximal parameter space indicated by the two parameter windows, because the available light energy is insufficient to sustain sinking phytoplankton beyond these limits. Thus, our results provide necessary but not sufficient conditions for bloom development by sinking phytoplankton.

Turbulence window: The turbulence window in stratified waters is similar to the turbulence window recently described for unstratified waters (Huisman et al. [25]). Basically, if turbulence levels in the upper water layer are too low, sinking rates may dominate over growth rates and turbulent mixing rates. In this case, there is no force that prevents sinking of the entire phytoplankton population. The sinking population literally falls out of the euphotic zone, and is lost. This mechanism underlies the existence of a minimal turbulence (Result 5). Its discovery can be traced back to at least the early work of Riley et al. [48]. Conversely, if turbulence levels are high, turbulent mixing rates dominate over growth rates and sinking rates. In this case, phytoplankton populations are uniformly mixed, and in deeply stratified waters they receive insufficient light to sustain a population. This mechanism underlies the existence of a maximal turbulence (Result 6). The maximal turbulence is compatible with the critical turbulence discovered by Huisman et al. [27]. For a given species, the turbulence windows in stratified and unstratified waters are identical, since, provided that the system is sufficiently deep, the mechanisms that underlie the turbulence window are independent of the length scale of the system, and hence independent of water-column depth and stratification depth.

Thermocline window: The thermocline window occurs in stratified waters with a turbulent upper water layer. In these waters, sinking losses over the thermocline are inversely

proportional to thermocline depth (Result 1). Therefore, if the thermocline is too shallow, export of sinking phytoplankton over the thermocline may exceed the integrated growth rate. This mechanism underlies the existence of a minimal thermocline depth (Result 3). The minimal thermocline depth is compatible with the critical parameter G derived by Condie and Bormans [10] and Condie [9]. The concept of a minimal thermocline depth is supported by field observations on the disappearance of sinking phytoplankton from shallow stratified waters (Reynolds et al. [47]; Visser et al. [62]; Condie and Bormans [10]; Diehl et al. [13]).

Conversely, if the thermocline is too deep, phytoplankton populations in the turbulent upper water layer receive insufficient light in the deeper parts of the water column and therefore integrated growth rates become too low. This mechanism underlies the existence of a maximal thermocline depth (Result 4). Conceptually, the maximal thermocline depth is similar to the critical depth of Sverdrup [58] (see also Platt et al. [43]). Lucas et al. [38] pointed out, however, that Sverdrup's critical depth does not consider losses of sinking phytoplankton over the thermocline. Our model formulation does include these sinking losses, and our analytical results confirm the finding of Lucas et al. that sinking losses over the thermocline may indeed seriously reduce the opportunities for bloom development of sinking phytoplankton in stratified waters (see Eq. (24)).

Blooms of sinking phytoplankton species are possible in stratified waters whose characteristics fall within the thermocline window. In fact, within the thermocline window, theory predicts a unimodal relationship between the population size of sinking phytoplankton and thermocline depth (Fig. 3B). Interestingly, this prediction is supported by a recent experiment in which different mixing depths were generated artificially in a freshwater lake dominated by sinking diatoms (Diehl et al. [13]), which indeed revealed a unimodal relation between phytoplankton biomass and mixed-layer depth.

Sinking velocity and export production: The turbulence window and thermocline window both decrease in size with increasing sinking velocity of the phytoplankton (Fig. 5). This revealed the existence of a maximal phytoplankton sinking velocity that can be sustained. Theory predicts that this maximal sinking velocity is inversely proportional to the background turbidity of the water column (Result 7). This makes sense intuitively: in order to proliferate, sinking phytoplankters must stay in the euphotic zone for a sufficiently long time. For a given sinking velocity, they remain longer in the euphotic zone if water clarity is high. As a consequence, clear waters can sustain phytoplankton species with high sinking velocities, whereas turbid waters can sustain only species with low sinking velocities (Fig. 7).

The dependence of the maximal sinking velocity on background turbidity may have an intriguing implication. Export production by sinking phytoplankton is the product of sinking velocity and population density. Theory predicts that, all else being equal, an increased background turbidity reduces both the maximal sinking velocity and the population density of phytoplankton. As a result, an increased background turbidity may shift the species composition from sinking species towards neutrally buoyant or motile species, and might drastically reduce export production of sinking phytoplankton (Result 8).

Conclusions: In conclusion, theory predicts that in both unstratified and stratified wa-

ters sinking phytoplankton can be sustained by means of a turbulence window. In contrast to unstratified waters, however, deep waters with a stratified upper mixed layer may also sustain sinking phytoplankton by means of a thermocline window. In this sense, stratification enhances growth opportunities for sinking phytoplankton. However, the concept of a minimal thermocline depth exists for sinking phytoplankton only, not for neutrally buoyant or buoyant phytoplankton. Also, all else being equal, the maximal thermocline depth is smaller for sinking phytoplankton than for neutrally buoyant and buoyant species. Hence, neutrally buoyant and buoyant phytoplankton will profit more from stratification than sinking phytoplankton. In this sense, under ample nutrient conditions, stratification is likely to tip the competitive balance in favor of neutrally buoyant and buoyant phytoplankton species. This interpretation is consistent with field observations, which often report changes in species composition from sinking species towards neutrally buoyant or buoyant species in response to water column stratification (Reynolds et al. [47]; Jones and Gowen [33]; Visser et al. [61]; Sherman et al. [53]; Irigoien et al. [30]).

A striking finding is the sensitivity of sinking phytoplankton species to the background turbidity of the water column. Intuitively, this sensitivity follows from two effects. First, background turbidity affects all phytoplankters by absorbing light that would otherwise have been available for phytoplankton photosynthesis. Second, light conditions deteriorate most rapidly for phytoplankters sinking through turbid waters. In short, the theory presented here predicts that sinking phytoplankton species are favored by unstratified clear waters.

Acknowledgements
We thank Manuel Arrayás, Kate Curwen, Ute Ebert, Jim Gillon, Nico Temme, and Anya Waite for helpful discussions on the topic.

Table 2: Sinking-velocity data of phytoplankton in oceans, estuaries, rivers, and lakes. Background turbidities were either given in the same reference as the sinking-velocity data, or else estimated from the sources indicated in the footn otes.

$v\ (m \cdot d^{-1})$	$K_{bg}\ (m^{-1})$	Species & water body	Reference
Oceans			
1.5	$0.11^{(1)}$	*Thalassiosira*, Pacific	Eppley et al. [17]
3	$0.11^{(1)}$	*Gonyaulax*, Pacific	Eppley et al. [17]
5	$0.11^{(1)}$	*Coscinodiscus w.*, Pacific	Eppley et al. [17]
7	$0.11^{(1)}$	*Coscinodiscus w.*, Pacific	Eppley et al. [17]
7.5	$0.11^{(1)}$	*Coscinodiscus w.*, Pacific	Eppley et al. [17]
9	$0.11^{(1)}$	*Coscinodiscus w.*, Pacific	Eppley et al. [17]
0.2	$0.15^{(2)}$	*Skeletonema*, North Pacific	Bienfang et al. [4]
0.5	$0.15^{(2)}$	*Chaetoceras*, North Pacific	Bienfang et al. [4]
1	$0.15^{(2)}$	*Ditylum*, North Pacific	Bienfang et al. [4]
2	$0.15^{(2)}$	*Coscinodiscus w.*, North Pacific	Bienfang et al. [4]
0.22	$0.03^{(3)}$	diatoms & dinoflagellates, Pacific Hawaii	Bienfang & Harrison [3]
0.96	$0.15^{(2)}$	diatoms, North Pacific	Bienfang & Harrison [3]
1.0	$0.11^{(1)}$	*Coscinodiscus c.*, Pacific	Granata, [22]
1.0	$0.25^{(4)}$	*Emiliania*, Gulf of Maine	Fritz & Balch [20]
0.30	$0.15^{(2)}$	*Emiliania*, North Pacific	LeCourt et al. [37]
0.60	$0.15^{(2)}$	*Actinocyclus*, North Pacific	Muggli et al. [42]
0.12	$0.15^{(2)}$	*Emiliania*, North Pacific	Muggli et al. [42]
0.5	0.105	diatoms, Southern Ocean	Boyd et al. [6]
1.3	0.055	diatoms, Southern Ocean	Boyd et al. [6]
25	$0.05^{(5)}$	*Ceratocorys*, Sargasso Sea	Zirbel et al. [63]
Estuaries & Rivers			
0.5	1.3	diatoms, San Francisco Bay	Koseff et al. [35]
0.8	0.92	diatoms, Lena River, Russia	Heiskanen & Keck [23]
0.9	0.44	*Aulocoseira*, Australia	Bormans & Webster [5]
Lakes			
0.31	0.54	*Cryptomonas e.*, Canada	Burns & Rosa [8]
0.32	0.54	*Cryptomonas m.*, Canada	Burns & Rosa [8]
0.07	0.54	*Rhodomonas*, Canada	Burns & Rosa [8]
0.27	0.54	*Fragilaria*, Canada	Burns & Rosa [8]
0.11	0.54	*Gomphosphaeria*, Canada	Burns & Rosa [8]
0.10	0.54	*Anabaena*, Canada	Burns & Rosa [8]
0.15	0.54	*Selenastrum*, Canada	Burns & Rosa [8]
0.18	0.54	*Closterium*, Canada	Burns & Rosa [8]
0.10	0.54	*Scenedesmus*, Canada	Burns & Rosa [8]
0.08	0.54	*Lagerhaemia*, Canada	Burns & Rosa [8]
0.7	$0.22^{(6)}$	*Asterionella* A, UK	Reynolds & Wiseman [45]
0.6	$0.22^{(6)}$	*Asterionella* B, UK	Reynolds & Wiseman [45]
0.8	$0.22^{(6)}$	*Fragilaria*, UK	Reynolds & Wiseman [45]
0.86	$1.5^{(7)}$	*Melosira*, Ireland	Gibson [21]
0.45	$1.5^{(7)}$	*Stephanodiscus*, Ireland	Gibson [21]
1.4	$0.25^{(8)}$	*Fragilaria*, Germany	Sommer [56]

v $(m \cdot d^{-1})$	K_{bg} (m^{-1})	Species & water body	Reference
1.2	$0.25^{(8)}$	*Asterionella*, Germany	Sommer [56]
0.65	$0.25^{(8)}$	*Stephanodiscus sp.*, Germany	Sommer [56]
0.033	$0.25^{(8)}$	*Stephanodiscus h.*, Germany	Sommer [56]
0.87	$0.25^{(8)}$	*Melosira*, Germany	Sommer [56]
0.38	$0.25^{(8)}$	*Staurastrum*, Germany	Sommer [56]
0.08	$0.25^{(8)}$	*Pandorina*, Germany	Sommer [56]
0.10	$0.25^{(8)}$	*Mougeotia*, Germany	Sommer [56]
0.04	$0.25^{(8)}$	*Aphanizomenon*, Germany	Sommer [56]
1.1	0.8	*Scenedesmus*, Netherlands	Visser et al [62]
1	0.23	*Mougeotia*, Italy	Salmaso [49]
6.5	0.23	*Flagilaria*, Italy	Salmaso [49]
0.25	0.61	diatoms, Germany	Diehl et al. [13]
0.31	0.84	diatoms, Germany	Diehl et al. [13]

(1) Table 6.1 of Kirk [34], Pacific off Mexico.
(2) Table 6.1 of Kirk [34], Eastern North Pacific.
(3) Table 6.1 of Kirk [34], Pacific off Hawaii.
(4) Townsend et al. [60].
(5) Table 6.1 of Kirk [34], Sargasso Sea.
(6) Reynolds et al. [46].
(7) Jewson [32].
(8) Tilzer [59].

References

[1] K.R. Arrigo, D.H. Robinson, D.L. Worthen, R.B. Dunbar, G.R. DiTullio, M. VanWoert, and M.P. Lizotte, *Phytoplankton community structure and the drawdown of nutrients and CO_2 in the Southern Ocean*, Science 283, 365-367 (1999).

[2] T. Berman and B. Shteinman, *Phytoplankton development and turbulent mixing in Lake Kinneret (1992-1996)*, Journal of Plankton Research 20, 709-726 (1998).

[3] P.K. Bienfang and J.P. Harrison, *Sinking-rate response of natural assemblages of temperate and subtropical phytoplankton to nutrient depletion*, Marine Biology 83, 293-300 (1984).

[4] P.K. Bienfang, J.P. Harrison, and L.M. Quarmby, *Sinking rate response to depletion of nitrate, phosphate and silicate in four marine diatoms*, Marine Biology 67, 295-302 (1982).

[5] M. Bormans and I.T. Webster, *Modelling the spatial and temporal variability of diatoms in the River Murray*, Journal of Plankton Research 21, 581-598 (1999).

[6] P.W. Boyd, A.J. Watson, C.S. Law, E.R. Abraham, T. Trull, R. Murdoch, D.C.E. Bakker, A.R. Bowie, K.O. Buesseler, H. Chang, M. Charette, P. Croot, K. Downing, R. Frew, M. Gall, M. Hadfield, J. Hall, M. Harvey, G. Jameson, J. LaRoche, M. Liddicoat, R. Ling, M.T. Maldonado, R.M. McKay, S. Nodder, S. Pickmere, R. Pridmore, S. Rintoul, K. Safi, P. Sutton, R. Strzepek, K. Tanneberger, S. Turner, A. Waite, and J. Zeldis, *A mesoscale phytoplankton bloom in the polar Southern Ocean stimulated by iron fertilization*, Nature 407, 695-702 (2000).

[7] P.N. Brown, G.D. Byrne, and A.C. Hindmarsh, *VODE: a variable-coefficient ODE solver*, SIAM Journal on Scientific and Statistical Computing 10, 1038-1051 (1989).

[8] N.M. Burns and F. Rosa, *In situ measurement of the settling velocity of organic carbon particles and 10 species of phytoplankton*, Limnology and Oceanography 25, 855-864 (1980).

[9] S.A. Condie, *Settling regimes for non-motile particles in stratified waters*, Deep-Sea Research 46, 681-699 (1999).

[10] S.A. Condie and M. Bormans, *The influence of density stratification on particle settling, dispersion and population growth*, Journal of Theoretical Biology 187, 65-75 (1997).

[11] W.T. De Nobel, H.C.P. Matthijs, E. von Elert, and L.R. Mur, *Comparison of the light-limited growth of the nitrogen-fixing cyanobacteria Anabaena and Aphanizomenon*, New Phytologist 138, 579-587 (1998).

[12] S. Diehl, *Phytoplankton, light, and nutrients in a gradient of mixing depths I: theory*, Ecology (2002) (in press).

[13] S. Diehl, S. Berger, R. Ptacnik, and A. Wild, *Phytoplankton, light, and nutrients in a gradient of mixing depths II: Field experiments*, Ecology (2002) (in press).

[14] G.R. DiTullio, J.M. Grebmeier, K.R. Arrigo, M.P. Lizotte, D.H. Robinson, A. Leventer, J.P. Barry, M.L. VanWoert, and R.B. Dunbar, *Rapid and early export of Phaeocystis antarctica blooms in the Ross Sea, Antarctica*, Nature 404, 595-598 (2000).

[15] P.L. Donaghay and T.R. Osborn, *Toward a theory of biological-physical control of harmful algal bloom dynamics and impacts*, Limnology and Oceanography 42, 1283-1296 (1997).

[16] U. Ebert, M. Arrayás, N.M. Temme, B.P. Sommeijer, and J. Huisman, *Critical conditions for phytoplankton blooms*, Bulletin of Mathematical Biology 63, 1095-1124 (2001).

[17] R.W. Eppley, R.W. Holmes, and J.D.H. Strickland, *Sinking rates of marine phytoplankton measured with a fluorometer*, Journal of Experimental Marine Biology in Ecology 1, 191-208 (1967).

[18] P.G. Falkowski, R.T. Barber, and V. Smetacek, *Biogeochemical controls and feedbacks on ocean primary production*, Science 281, 200-206 (1998).

[19] P.J.S. Franks and C. Chen, *A 3-D prognostic numerical model study of the Georges bank ecosystem. Part II: biological-physical model*, Deep-Sea Research II 48, 457-482 (2001).

[20] J.J. Fritz and W.M. Balch, *A light-limited continuous culture study of Emiliania huxleyi: determination of coccolith detachment and its relevance to cell sinking*, Journal of Experimental Marine Biology in Ecology 207, 127-147 (1996).

[21] C.E. Gibson, *Sinking rates of planktonic diatoms in an unstratified lake: a comparison of field and laboratory observations*, Freshwater Biology 14, 631-638 (1984).

[22] T.C. Granata, *Diel periodicity in growth and sinking rates of the centric diatom Coscinodiscus concinnus*, Limnology and Oceanography 36, 132-139 (1991).

[23] A.S. Heiskanen and A. Keck, *Distribution and sinking rates of phytoplankton, detritus, and particulate biogenic silica in the Laptev Sea and Lena River (Arctic Siberia)*, Mar. Chem. 53, 229-245 (1996).

[24] J. Huisman, *Population dynamics of light-limited phytoplankton: microcosm experiments*, Ecology 80, 202-210 (1999).

[25] J. Huisman, M. Arrayás, U. Ebert, and B.P. Sommeijer, *How do sinking phytoplankton species manage to persist?*, American Naturalist (2002) (in press).

[26] J. Huisman, R.R. Jonker, C. Zonneveld, and F.J. Weissing, *Competition for light between phytoplankton species: experimental tests of mechanistic theory*, Ecology 80, 211-222 (1999).

[27] J. Huisman, P. van Oostveen, and F.J. Weissing, *Critical depth and critical turbulence: two different mechanisms for the development of phytoplankton blooms*, Limnology and Oceanography 44, 1781-1788 (1999).

[28] J. Huisman and B.P. Sommeijer, *Simulation techniques for the population dynamics of sinking phytoplankton in light-limited environments*, Report MAS-R0201, CWI, Amsterdam (2002).

[29] J. Huisman and F.J. Weissing, *Light-limited growth and competition for light in well-mixed aquatic environments: an elementary model*, Ecology 75, 507-520 (1994).

[30] X. Irigoien, R.P. Harris, R.N. Head, and D. Harbour, *North Atlantic oscillation and spring bloom phytoplankton composition in the English Channel*, Journal of Plankton Research 22, 2367-2371 (2000).

[31] A.D. Jassby and T. Platt, *Mathematical formulation of the relationship between photosynthesis and light for phytoplankton*, Limnology and Oceanography 21, 540-547 (1976).

[32] D.H. Jewson, *Light penetration in relation to phytoplankton content of the euphotic zone in Lough Neagh, North Ireland*, Oikos 28, 74-83 (1977).

[33] K.J. Jones and R.J. Gowen, *Influence of stratification and irradiance regime on summer phytoplankton composition in coastal and shelf seas of the British Isles (UK)*, Estuarine Coastal and Shelf Science 30, 557-568 (1990).

[34] J.T.O. Kirk, *Light and Photosynthesis in Aquatic Ecosystems*, 2nd ed., Cambridge Univ. Press, Cambridge (1994).

[35] J.R. Koseff, J.K. Holen, S.G. Monismith, and J.E. Cloern, *Coupled effects of vertical mixing and benthic grazing on phytoplankton populations in shallow, turbid estuaries*, Journal of Marine Research 51, 843-868 (1993).

[36] M.L. Lauria, D.A. Purdie, and J. Sharples, *Contrasting phytoplankton distributions controlled by tidal turbulence in an estuary*, Journal of Marine Systems 21, 189-197 (1999).

[37] M. LeCourt, D.L. Muggli, and P.J. Harrison, *Comparison of growth and sinking rates of non-coccolith and coccolith-forming strains in Emiliania huxleyi (Prymnesiophyceae) grown under different irradiances and nitrogen sources*, J. Phycol. 32, 17-21 (1996).

[38] L.V. Lucas, J.E. Cloern, J.R. Koseff, S.G. Monismith, and J.K. Thompson, *Does the Sverdrup critical depth model explain bloom dynamics in estuaries?*, Journal of Marine Research 56, 375-415 (1998).

[39] K.H. Mann and J.R.N. Lazier, *Dynamics of Marine Ecosystems: Biological-Physical Interactions in the Oceans*, 2nd ed., Blackwell, Oxford (1996).

[40] D. Martin and R. Nokes, *Crystal settling in a vigorously convecting magma chamber*, Nature 332, 534-536 (1988).

[41] J. Monod, *La technique de culture continue, théorie et applications*, Annales de l'Institut Pasteur (Paris) 79, 390-410 (1950).

[42] D.L. Muggli, M. LeCourt, and P.J. Harrison, *Effects of iron and nitrogen source on the sinking rate, physiology and metal composition of an oceanic diatom from the subarctic Pacific*, Mar. Ecol. Prog. Ser. 132, 215-227 (1996).

[43] T. Platt, D.F. Bird, and S. Sathyendranath, *Critical depth and marine primary production*, Proceedings of the Royal Society of London, B. 246, 205-217 (1991).

[44] C.S. Reynolds, M.L. White, R.T. Clarke, and A.F. Marker, *Suspension and settlement of particles in flowing water: comparison of the effects of varying water depth and velocity in circulating channels*, Freshwater Biology 24, 23-24 (1990).

[45] C.S. Reynolds and S.W. Wiseman, *Sinking losses of phytoplankton in closed limnetic systems*, Journal of Plankton Research 4, 489-522 (1982).

[46] C.S. Reynolds, S.W. Wiseman, and M.J.O. Clarke, *Growth- and loss-rate responses of phytoplankton to intermittent artificial mixing and their potential application to the control of planktonic algal biomass*, J. Appl. Ecol. 21, 11-39 (1984).

[47] C.S. Reynolds, S.W. Wiseman, B.M. Godfrey, and C. Butterwick, *Some effects of artificial mixing on the dynamics of phytoplankton populations in large limnetic exclosures*, Journal of Plankton Research 5, 203-234 (1983).

[48] G.A. Riley, H. Stommel, and D.F. Bumpus, *Quantitative ecology of the plankton of the western North Atlantic*, Bulletin of the Bingham Oceanographic Collection 12, 1-169 (1949).

[49] N. Salmaso, *Factors affecting the seasonality and distribution of cyanobacteria and prochlorophytes: a case study from the large lakes south of the Alps, with special reference to Lake Garda*, Hydrobiologica 438, 43-63 (2000).

[50] C. Sancetta, T. Villareal, and P.G. Falkowski, *Massive fluxes of rhizosolenoid diatoms: a common occurrence?*, Limnology and Oceanography 36, 1452-1457 (1991).

[51] J.L. Sarmiento, T.M.C. Hughes, R.J. Stouffer, and S. Manabe, *Simulated response of the ocean carbon cycle to anthropogenic climate warming*, Nature 393, 245-249 (1998).

[52] J. Sharples and P. Tett, *Modelling the effect of physical variability on the midwater chlorophyll maximum*, Journal of Marine Research 52, 219-238 (1994) .

[53] B.S. Sherman, I.T. Webster, G.J. Jones, and R.L. Oliver, *Transitions between Aulacoseira and Anabaena dominance in a turbid river weir pool*, Limnology and Oceanography 43, 1902-1915 (1998).

[54] N. Shigesada and A. Okubo, *Analysis of the self-shading effect on algal vertical distribution in natural waters*, Journal of Mathematical Biology 12, 311-326 (1981).

[55] I.R. Smith, *A simple theory of algal deposition*, Freshwater Biology 12, 445-449 (1982).

[56] U. Sommer, *Sedimentation of principle phytoplankton species in Lake Constance*, Journal of Plankton Research 6, 1-14 (1984).

[57] E.T. Sundquist, *The global carbon dioxide budget*, Science 259, 934-941 (1993).

[58] H.U. Sverdrup, *On conditions for the vernal blooming of phytoplankton*, Journal du Conseil Permanent International pour l'Exploration de la Mer 18, 287-295 (1953).

[59] M.M. Tilzer, *The importance of fractional light absorption by photosynthetic pigments for phytoplankton productivity in Lake Constance*, Limnology and Oceanography 28, 833-846 (1983).

[60] D.W. Townsend, M.D. Keller, M.E. Sieracki, and S.G. Ackleson, *Spring phytoplankton blooms in the absence of vertical water column stratification*, Nature 360, 59-62 (1992).

[61] P.M. Visser, B.W. Ibelings, B. van der Veer, J. Koedood, and L.R. Mur, *Artificial mixing prevents nuisance blooms of the cyanobacterium Microcystis in Lake Nieuwe Meer, The Netherlands*, Freshwater Biology 36, 435-450 (1996).

[62] P.M. Visser, L. Massaut, J. Huisman, and L.R. Mur, *Sedimentation losses of Scenedesmus in relation to mixing depth*, Archiv für Hydrobiologie 136, 289-308 (1996).

[63] M.J. Zirbel, F. Veron, and M.I. Latz, *The reversible effect of flow on the morphology of Ceratocorys horrida (Peridiniales, Dinophyta)*, J. Phycol. 36, 46-58 (2000).